Equilibrium in the clinoptilolite-H₂O system

J. William Carey and David L. Bish

EES-1/MS D469, Los Alamos National Laboratory, Los Alamos, New Mexico 87545, U.S.A.

Abstract

A thermodynamic formulation for the sorption of H_2O in clinoptilolite has been obtained from analysis of equilibrium data collected by thermogravimetry on near end-member Ca-, Na-, and K-exchanged natural clinoptilolite (Fish Creek Mountains, Nevada). Temperature and pressure of the experiments ranged from 25 to 250 °C and 0.2 to 35 mbar H_2O vapor pressure. Equilibrium of three clinoptilolite species was successfully formulated with the following expression for the Gibbs free energy of hydration as a function of temperature and pressure:

$$\Delta\mu_{Hy}/T = \Delta\mu_{Hy}^0/T_0 + \Delta\overline{H}_{Hy}^0(1/T - 1/T_0) - 3R[\ln(T/T_0) + (T_0/T - 1)]$$
$$+ R \ln[\theta/(1 - \theta)P] + \frac{W_1}{T}\theta + \frac{W_2}{T}\theta^2$$

where R is the gas constant, P is the vapor pressure of H_2O, W_1 and W_2 are the excess mixing parameters, and θ is the ratio $H_2O/(\text{maximum } H_2O)$ with maximum water contents for the K, Na, and Ca end-members of 13.49, 15.68, and 16.25 wt%, respectively. The molar Gibbs free energy of hydration for calcium, sodium, and potassium clinoptilolite is -36.13 ± 3.02, -29.68 ± 3.77, and -25.53 ± 1.37 kJ/mol H_2O, respectively. The molar enthalpy of hydration for these phases is -76.92 ± 2.88, -74.19 ± 3.46, and -67.78 ± 1.25 kJ/mol H_2O.

The thermodynamic formulation is applied to the occurrence of clinoptilolite at Yucca Mountain, Nevada, where the proposed emplacement of nuclear waste would lead to heating of clinoptilolite-bearing tuffs. Rock units with abundant clinoptilolite (or by analogy other hydrous phases) would remain significantly cooler than units with anhydrous minerals and would evolve a substantial volume of water.

Introduction

Zeolites are hydrous framework silicates that incorporate molecular H_2O by sorption into a porous crystal structure. It is of considerable interest to obtain a thermodynamic description of this sorption process for the purpose of evaluating the effect of H_2O vapor pressure on zeolite stability and characterizing the amount of water and energy consumed or liberated by zeolites as a function of changes in pressure and temperature.

Zeolite + H_2O equilibria are important in a variety of environments. These include diagenetic and low-grade metamorphic occurrences in which zeolite stability may be used to determine the conditions of metamorphism; pollution abatement in which zeolites are present naturally or placed in the environment to act as sorptive barriers to contaminant migration; and industrial settings in which zeolites are used as catalysts, molecular sieves, and cation exchangers.

This study focuses on the zeolite clinoptilolite [ideally $(Na,K,\frac{1}{2}Ca)_6Al_6Si_{30}O_{72} \cdot 20H_2O$] and presents experimental results that allow determination of the thermodynamics of hydration. Clinoptilolite forms in low-temperature systems by reaction among aqueous fluids and unstable

aluminosilicates such as glass, opal, feldspars, etc. (e.g., Gottardi and Galli 1985). Typical genetic environments for clinoptilolite include tuffs and tuffaceous sediments, saline lakes, and deep-sea sediments.

The primary motivation for this work is the presence of a considerable quantity of clinoptilolite at Yucca Mountain, Nevada, a potential repository for high-level radioactive waste. In the evaluation of the site suitability, a significant concern is the response of clinoptilolite to the thermal energy generated by the stored nuclear waste. It is anticipated that clinoptilolite will dehydrate and consume thermal energy, and these experiments are designed to provide a quantitative basis for predicting the water content, the amount of water released, and the thermal energy consumed by clinoptilolite as a function of thermal history at Yucca Mountain. These results can be used to provide a more accurate thermohydrologic model for the evolution of Yucca Mountain.

Clinoptilolite is characterized by a sheetlike organization of the aluminosilicate framework into layers perpendicular to the b axis (e.g., Alberti 1975). There are two channels defined by ten- and eight-membered tetrahedral rings parallel to c, which intersect a channel defined by eight-membered rings parallel to the a axis. The intersec-

tion of the channels defines two cages of unequal size. Exchangeable cations are located on a mirror plane through the center of the cages and are solvated by H_2O in irregular polyhedra (e.g., Armbruster and Gunter 1991). Armbruster and Gunter's (1991) study of dehydration revealed a complex process of H_2O loss and structural rearrangement coupled with exchangeable-cation movement. The pattern of H_2O loss was consistent with the existence of a range of energetic sites for H_2O, with the lowest energy sites located farthest from monovalent cations.

Several previous investigations of the thermodynamic properties of clinoptilolite include: a calorimetric study that provided the enthalpy of formation of a hydrous and anhydrous clinoptilolite from Malheur County, Oregon (Johnson et al. 1991); a calorimetric study of the molar enthalpy of hydration of synthetic sodium clinoptilolite (Barrer and Cram 1971); a gravimetric study of the equilibrium H_2O content of several natural clinoptilolite samples at 20 °C (Yamanaka et al. 1989); and two structural and gravimetric studies of the isotypic zeolite, heulandite (Barrer and Fender 1961; Simonot-Grange 1979). Unfortunately, these studies do not provide a complete thermodynamic formulation of the hydration properties of clinoptilolite or heulandite. Consequently, a set of phase-equilibrium experiments was performed to derive the thermodynamics of hydration in clinoptilolite.

Cation-exchanged clinoptilolite was equilibrated with H_2O vapor in a thermogravimetric analyzer. The data consist of the equilibrium H_2O content (mass) at a known temperature and partial pressure of H_2O. A thermodynamic analysis of these data yields an equation of state for zeolitic H_2O in clinoptilolite. The equation of state permits prediction of the equilibrium H_2O content in clinoptilolite as a function of temperature and H_2O vapor pressure and the calculation of the thermodynamic properties of H_2O in clinoptilolite, including the integral and partial molar enthalpies of hydration.

EXPERIMENTAL METHODS

Clinoptilolite samples were obtained from Minerals Research, reference no. 27054, from a clinoptilolite-rich tuff from Fish Creek Mountains, Nevada. The clinoptilolite was purified by disaggregation with an ultrasonic probe and gravitational settling in deionized water (Chipera et al. 1993). Samples were extracted from the 15 min settling fraction, following the removal of material that settled within 30 s. The samples correspond, approximately, to the 10 μm size fraction. Nearly pure clinoptilolite was confirmed by X-ray powder diffraction, with minor impurities (<5% total) of quartz, alkali feldspar, and calcite.

The natural material was cation exchanged in 1 m sodium, potassium, and calcium chloride solutions at room temperature. The exchange solution was replaced 9–16 times with exchange periods ranging from 5 to 400 h. The resulting chemical compositions, obtained by J. Husler of the University of New Mexico using X-ray fluores-

TABLE 1. Chemical analyses of purified natural and cation-exchanged clinoptilolite from Fish Creek Mountains, Nevada

Oxides (wt%)	Natural	Na-exchanged	K-exchanged	Ca-exchanged*
SiO₂	64.25	65.01	63.77	
Al₂O₃	12.57	12.81	12.76	
Fe₂O₃	0.51	0.19	0.3	
FeO	n.d.	n.d.	n.d.	
MgO	1.02	0.43	0.37	0.78
CaO	3.07	0.24	0.27	4.46
Na₂O	0.92	5.75	0.31	0.192
K₂O	3.31	1.31	10.05	1.44
TiO₂	0.076	0.061	0.061	
P₂O₅	0.025	0.017	0.018	
MnO	0.011	0.007	0.006	
H₂O (LOI)**	14.51	14.19	12.21	
Total	100.272	100.015	100.125	

Note: Natural: $(Na_{0.86}K_{1.91}Ca_{1.49}Mg_{0.69})(Al_{6.70}Fe_{0.17}Si_{29.04})O_{72} \cdot 21.9H_2O$. Na-exchanged: $(Na_{6.78}K_{0.75}Ca_{0.12}Mg_{0.29})(Al_{6.78}Fe_{0.06}Si_{29.20})O_{72} \cdot 21.3H_2O$. K-exchanged: $(Na_{0.27}K_{5.84}Ca_{0.13}Mg_{0.25})(Al_{6.85}Fe_{0.10}Si_{29.04})O_{72} \cdot 18.5H_2O$. Ca-exchanged $(Na_{0.18}K_{0.90}Ca_{2.34}Mg_{0.57})(Al_{6.70}Fe_{0.17}Si_{29.04})O_{72} \cdot nH_2O$. Framework composition of the Ca-exchanged clinoptilolite assumed to be that of the natural clinoptilolite. H_2O content not determined; n.d. = not detected.
  * Only exchangeable cations were analyzed.
  ** Loss on ignition.

cence and atomic absorption, are given in Table 1. On a charge basis, the Na exchange was 76% complete, the K exchange 85% complete, and the Ca exchange 68% complete.

The equilibration measurements were made using a DuPont 951 thermogravimetric analyzer (TGA). Approximately 15–18 mg of sample was placed on the calibrated balance. A calibrated thermocouple recorded the temperature of the sample. Partial pressure of H_2O was controlled and delivered to the sample by mixing dry nitrogen gas with water-saturated nitrogen gas using two mass-flow controllers. A total gas flux of 100 cm³/min was maintained during the experiments. The relative humidity of the gas mixture was measured with a calibrated Vaisala 36B humidity probe immediately before the mixture entered the TGA. The geometry of the TGA is such that the gas flows horizontally over the sample, helping to minimize thermally induced gas-composition gradients. The relative humidity and temperature measurements were converted to partial pressure of H_2O using the data of Haar et al. (1984).

DATA

Experimental data were collected using two methods. The first technique involved holding the partial pressure of H_2O constant while varying the sample temperature from 25 to 220 or 250 °C in a sequence of isothermal stages. The samples were held at temperature for 60–300 min to allow equilibration. Measurements were made in a sequence of both rising and falling isotherms to assess the degree of reversibility. Typical results are illustrated in Figure 1 for calcium clinoptilolite at approximately 2 mbar H_2O vapor pressure. Little hysteresis was detected in these measurements within experimental precision (see below).
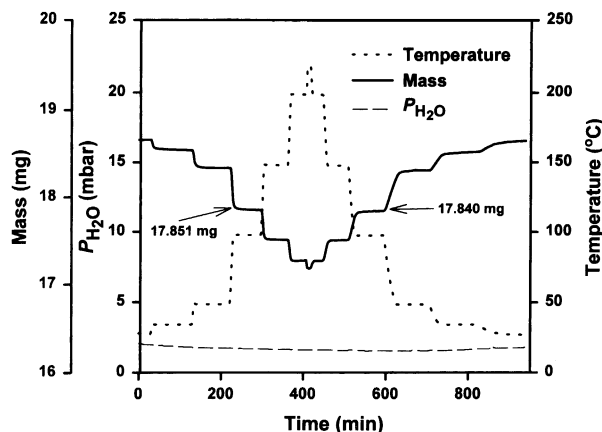
FIGURE 1. Results of a single experiment on calcium clinoptilolite conducted in a series of isothermal stages from 25 to 220 °C at approximately constant H_2O vapor pressure of 2 mbar. Two mass measurements are indicated at 100 °C to illustrate the degree of reversibility attained under conditions of falling and rising temperature.

FIGURE 3. Room-temperature equilibration data for sodium clinoptilolite at 24–25 and 26–27 °C (with saturation pressures of 30.8 and 34.6 mbar, respectively). Error bars correspond to the estimated one standard deviation uncertainty in the measurements. The effect of condensation on the apparent mass of H_2O in sodium clinoptilolite is evident in the rapid increase as the saturation pressure is approached.

The second method involved holding the temperature constant while the partial pressure of H_2O was varied between approximately 0.2 and 30 mbar in a sequence of isobaric stages. Samples were held at constant partial pressure for 60–100 min before the next partial-pressure interval. Measurements were made during both rising and falling isobars (Fig. 2).

The Na-exchanged clinoptilolite displayed irreversible behavior, with a small but definite loss of H_2O sorption capacity following heating to temperatures as low as 250 °C. Both the Ca- and K-exchanged samples retained reversible behavior to 250 °C. The irreversible sorption of H_2O in sodium clinoptilolite at $T > 220$ °C is consistent with observations made on the structural effects of short-

and long-term heating experiments. Bish (1984) found a much greater decrease in the molar volume of sodium clinoptilolite upon short-term (~ 1 h) heating to 300 °C than for calcium or potassium clinoptilolite. In addition, Bish (1990) found that sodium clinoptilolite, in contrast to calcium and potassium clinoptilolite, underwent an irreversible structural transformation when heated to 200 °C for times on the order of months.

Data were obtained at 25, 34, 48, 74, 98, 148, 198, and 218 °C for sodium, calcium, and potassium clinoptilolite and also at 248 °C for calcium and potassium clinoptilolite for H_2O vapor pressures between about 0.2 and 35 mbar. The range of H_2O vapor pressure was limited by the lowest, accurate readings of the humidity probe and the saturation pressure of water at room temperature.

Sources of error in the data include a one standard deviation uncertainty in the mass of H_2O of approximately 2–3%; an uncertainty in the measurement of H_2O vapor pressure of about 2%; and an uncertainty in temperature of approximately 1–3 °C (Fig. 3). Most of the scatter observed in the data may be accounted for by these errors.

As saturation pressures were approached, the apparent mass of H_2O in clinoptilolite rose rapidly for both the 25 and 27 °C data sets (Fig. 3). This is attributed to condensation rather than intracrystalline absorption. Consequently, it was necessary to extrapolate the data in Figure 3 to obtain a value of the sorption capacity at saturation pressures. Generally, such an extrapolation indicates the maximum sorption capacity of zeolite and is useful in idealized models of mixing properties of zeolites. The maximum H_2O-sorption capacities obtained by extrapolation for the three clinoptilolite samples are as follows: Na-exchanged 15.68 wt%, Ca-exchanged 16.25 wt%, and K-exchanged 13.49 wt%.
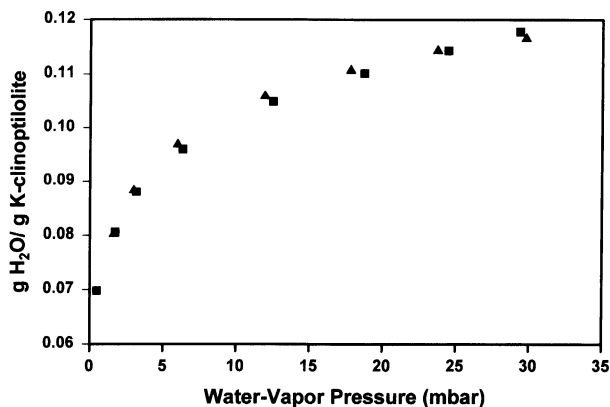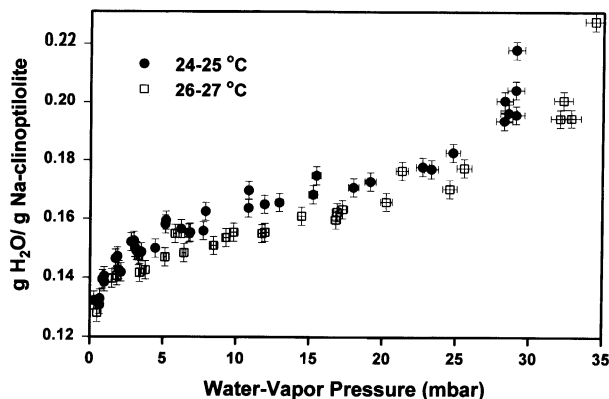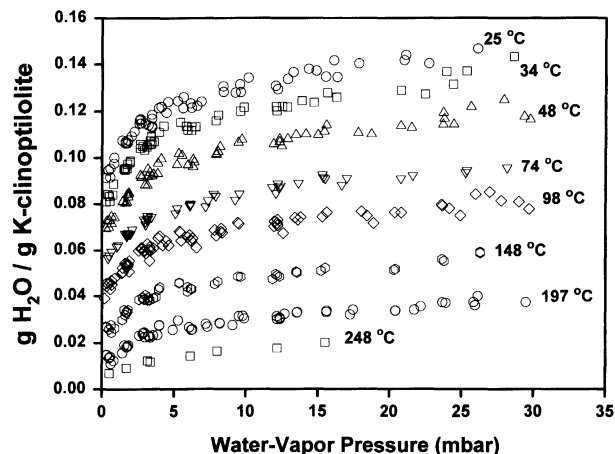

FIGURE 2. Results of a single experiment on potassium clinoptilolite conducted at 48 °C in a series of isobaric stages starting at approximately 30 mbar H_2O vapor pressure, decreasing to 0.5 (squares), and then increasing back to 30 mbar (triangles). The data were collected along 60 min isobars.

FIGURE 4. Summary of the experimental data for potassium clinoptilolite between 25 and 248 °C and 0.2 and 35 mbar H₂O vapor pressure collected in isothermal and isobaric stages.

FIGURE 5. Summary of the experimental data for calcium clinoptilolite for the equilibrium constant, ln K [defined as ln(x/P)], vs. x, where x is in grams of H₂O per grams of calcium clinoptilolite and P is in bars.

A restricted range of H₂O contents was obtainable at any single temperature, as illustrated for K-exchanged clinoptilolite (Fig. 4). This results from the highly energetic nature of the clinoptilolite-H₂O system in which clinoptilolite retains considerable water even at low partial pressure, and because the experimental apparatus did not allow the application of H₂O vapor pressure in excess of about 35 mbar (room-temperature, water vapor saturation). This situation complicated the determination of the thermodynamics of hydration because the complete range of H₂O contents was not accessible at any single temperature.

The relationship of the equilibrium constant to H₂O content provides a sensitive method of examining the data. Data for Ca-exchanged clinoptilolite are illustrated in Figure 5 with the equilibrium constant, ln K, defined by the following relations describing the sorption of H₂O from the vapor (V) to clinoptilolite (Cpt):

$$H_2O^V \rightleftharpoons H_2O^{Cpt} \qquad (1)$$

$$\ln K = \ln\left(\frac{x}{P}\right) \qquad (2)$$

where x is the H₂O content of clinoptilolite in grams of H₂O per grams of anhydrous clinoptilolite, and P is the H₂O vapor pressure in bars. Figure 5 illustrates several important points. First, the fact that isothermal values of the equilibrium constant are not constant reveals non-ideality in the system and indicates that the equilibrium constant is a function of the H₂O content, x. Second, curvature in the isothermal arrays of ln K values indicates that the equilibrium constant is a function of at least x^2. And third, the similar and regular behavior of the trend in the isothermal data as temperature increases from 25 to 248 °C and H₂O content decreases from saturation to nearly zero suggests that a relatively simple energetic model can describe hydrous clinoptilolite.
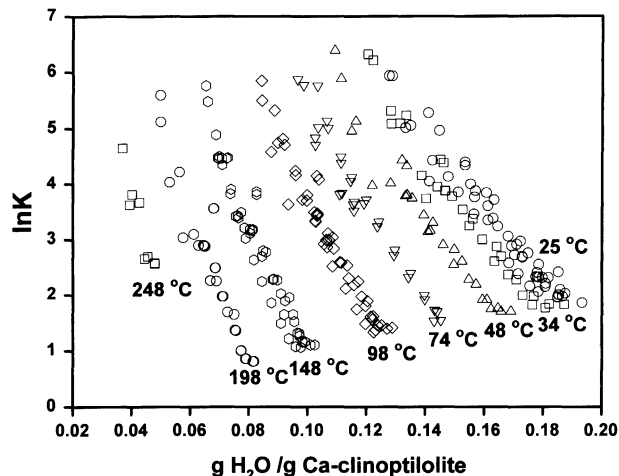
ANALYSIS

Thermodynamic relations

The thermodynamic properties of H₂O in clinoptilolite were obtained by a thermodynamic analysis of equilibrium data in the clinoptilolite-H₂O system. At equilibrium the chemical potential of H₂O in the vapor phase equals that in hydrous clinoptilolite:

$$\mu^V_{H_2O} = \mu^{Cpt}_{H_2O}. \qquad (3)$$

Expanding this equation to illustrate standard states and the equilibrium constant yields

$$\Delta\mu_{Hy} = \Delta\mu^0_{Hy} + RT \ln\left(\frac{a^{Cpt}_{H_2O}}{f^V_{H_2O}}\right) = \Delta\mu^0_{Hy} + RT \ln K \qquad (4)$$

in which the subscript Hy refers to the hydration reaction of Equation 1. The standard state for H₂O is the ideal gas at the temperature of interest and 1 bar. Data were analyzed with the assumption of two standard states for the sorbed H₂O in clinoptilolite. In the first, activity is represented by

$$a^{Cpt}_{H_2O} = \gamma_1 \theta \qquad (5)$$

where θ equals (H₂O content)/(maximum H₂O content), and γ_1 is the activity coefficient for θ. Here, the standard state corresponds to a Henry's law extrapolation to complete saturation of clinoptilolite at the temperature of interest. In the second case,

$$a^{Cpt}_{H_2O} = \gamma_2 x \qquad (6)$$

where x equals grams of H₂O per gram of dry clinoptilolite. In this case, the standard state corresponds to the hypothetical condition in which $\gamma_2 = x = 1$ at the temperature of interest.

The use of θ is well established in the zeolite literature

(e.g., Barrer 1978). Its utility lies in the simplified treatment of mixing in which H_2O molecules mix on a distinct number of sites given by the maximum amount of H_2O observed at saturation. In general, the number of sites is difficult to predict from single-crystal structure refinements because of ambiguity in site assignments, positional disorder of H_2O, and difficulty in accounting for the effect of differences in exchangeable cations. Nonetheless, an idealized maximum H_2O content of 26 molecules per 72 framework O atoms is suggested by X-ray structure refinements such as that by Armbruster and Gunter (1991). This value contrasts with the maximum H_2O contents determined in this study for the Ca-, Na-, and K-exchanged samples of 24.8, 23.9, and 20.8 H_2O pfu, respectively.

The activity expression for ideal sorption of H_2O in terms of θ is

$$a_{H_2O}^{Cpt}(ideal) = \frac{\theta}{(1 - \theta)} \qquad (7)$$

which is equivalent to ideal Langmuir sorption (e.g., Barrer 1978). This was found to be a good, first approximation to the mixing properties of sorbed species.

However, the use of θ also creates uncertainties. First, it is difficult to determine accurately the maximum amount of H_2O (x_{max}) in a zeolite because of condensation as the saturation pressure is approached (cf. Fig. 3 and Discussion). An alternative is to treat x_{max} as an additional fitting parameter. Unfortunately, regression of x_{max} is difficult because it is precisely at the conditions near saturation that accurate values of the H_2O content are necessary. A second difficulty is that x_{max} is generally a function of temperature and pressure. We are aware of no measurements of this dependence for the case of sorbed H_2O. However, Barrer and Davies (1970) suggested that this dependence is similar to the thermal expansion and compressibility of the liquid (i.e., the sorbed gas is approximated by a liquid, and any change in its partial molar volume should affect x_{max}). They documented the temperature dependence of N_2, CO_2, Ar, and several other gases in hydrogen chabazite. In addition, Bish (1984) demonstrated that the clinoptilolite structure contracts during dehydration (from 1.6 to 8.4% depending on the exchangeable cation), which would probably affect the value of x_{max}.

An alternative formulation of the activity that eliminates the need for an assumed, constant value of x_{max} makes use of a compositional variable, called x in Equations 2 and 6, with units of grams of H_2O per grams of anhydrous clinoptilolite. The disadvantage of this formulation is that ideal mixing (if it exists) would not be as accurately characterized. A comparative analysis using x and θ would ensure that the most appropriate mixing model is used.

The thermodynamic data necessary to apply Equation 4 as a function of temperature and pressure are shown by the function μ/T for which the total differential at constant composition may be expressed as

$$d\left(\frac{\mu}{T}\right) = \overline{H}d\left(\frac{1}{T}\right)_P + \frac{\overline{V}}{T} d(P)_{1/T} \qquad (8)$$

leading to the expression

$$\frac{\Delta\mu_{Hy}}{T} = \frac{\Delta\mu_{Hy}^0}{T_0} + \Delta\overline{H}_{Hy}^0\left(\frac{1}{T} - \frac{1}{T_0}\right)$$

$$- \int \frac{1}{T^2} \int \Delta\overline{Cp} \, dT \, dT$$

$$+ \int \frac{\overline{V}_{H_2O}^{0,Cpt}}{T} dP + R \ln K$$

$$= 0 \qquad (9)$$

where $\overline{V}_{H_2O}^{0,Cpt}$ is the standard-state, partial molar volume of H_2O in clinoptilolite, and T_0 is the reference-state temperature.

Nonideality in the clinoptilolite-H_2O system was assumed to be represented by a polynomial expansion of the H_2O content, with separate results obtained for each cation-exchanged clinoptilolite. For activities expressed in terms of θ or x, the expressions used were

$$a_{H_2O}^{Cpt} = \frac{\theta}{(1 - \theta)} \exp(W_1\theta + W_2\theta^2 + \ldots) \qquad (10)$$

$$a_{H_2O}^{Cpt} = x \exp(W_1x + W_2x^2 + \ldots) \qquad (11)$$

where W_1, W_2, etc., are temperature-independent coefficients. The degree of the polynomial was determined by analysis of the data. Other polynomial-type expressions were examined that also included temperature-dependent terms. Although some of these provided reasonable fits to the data, the partial molar enthalpies of hydration were unreasonably large near saturation.

Data analysis

The thermodynamic properties of H_2O in clinoptilolite were obtained by multiple linear regression using Equation 9 in combination with one of the activity expressions (Eqs. 10 and 11). Several simplifying assumptions were made. The energetic contributions of the change in volume upon dehydration were ignored (cf. Bish 1984). The present experiments were conducted at a total pressure of approximately 1 bar, for which the maximum expected energetic effect is on the order of 10 J/mol clinoptilolite (72 O-atom basis). The difference in heat capacity between H_2O in the gas and that in the sorbed phase was assumed to be constant with a value given by 3R, where R is the gas constant (Johnson et al. 1991; Carey 1993). This represents a relatively small energetic contribution with a maximum likely error of 600 J/mol H_2O at 250 °C decreasing to 0 at 25 °C (these error estimates correspond to an uncertainty of ±R). The data used in the regression were limited to a maximum H_2O content determined by extrapolation at 25 °C (Fig. 3), thus excluding all data judged to reflect condensation effects. With these considerations, the expression for the Gibbs free

TABLE 2. Summary of linear regression results for the model given by Equations 13 (activity based on θ) and 14 (activity based on x)

Parameter	Ca-exchanged		Na-exchanged		K-exchanged	
	θ model	x model	θ model	x model	θ model	x model
A (no units)	−16.4556	−18.9911	−17.9565	−20.8367	−17.0370	−19.4127
B (K)	14490.1	14589.4	11978.3	12394.2	10966.8	11154.7
C (K)	−16485.7	−80574.9	−8685.37	−45356.6	−8978.15	−58581.1
D (K)	9012.63	195735	3862.03	76556.2	5018.52	180255
r^2	0.9393	0.9345	0.9108	0.9031	0.9747	0.9587
Std. errors	0.34	0.33	0.45	0.41	0.23	0.25
No. of data	285	285	243	243	424	424

energy of hydration using the activity model for θ becomes

$$\frac{\Delta\mu_{Hy}}{T} = \frac{\Delta\mu^0_{Hy}}{T_0} + \Delta\overline{H}^0_{Hy}\left(\frac{1}{T} - \frac{1}{T_0}\right)$$

$$- 3R\left[\ln\left(\frac{T}{T_0}\right) + \left(\frac{T_0}{T} - 1\right)\right]$$

$$+ R\ln K + \frac{W_1}{T}\theta + \frac{W_2}{T}\theta^2 + \ldots$$

$$= 0. \tag{12}$$

The number of unknown parameters in Equation 12 depends on the degree of the nonideality polynomial (e.g., for a second-order polynomial, four parameters would be used to fit the data). For multiple linear regression, Equation 12 was rearranged and condensed to isolate the parameters as

$$\ln\left[\frac{\theta}{(1-\theta)P}\right] - 3\left[\ln\left(\frac{T}{T_0}\right) + \left(\frac{T_0}{T} - 1\right)\right]$$

$$= A + \frac{B}{T} + \frac{C}{T}\theta + \frac{D}{T}\theta^2 + \ldots \tag{13}$$

$$\ln\left(\frac{x}{P}\right) - 3\left[\ln\left(\frac{T}{T_0}\right) + \left(\frac{T_0}{T} - 1\right)\right]$$

$$= A + \frac{B}{T} + \frac{C}{T}x + \frac{D}{T}x^2 + \ldots \tag{14}$$

Results

Multiple linear regressions for sodium, potassium, and calcium clinoptilolite indicate that a second-order polynomial is sufficient to characterize the nonideality of H_2O in clinoptilolite (Table 2). The regressions for both activity models have r^2 values greater than 0.9. As an estimate of the precision of the fit, the standard errors of the predicted values of $\ln K$ are given in Table 2.

The two activity models result in only small differences in derived thermodynamic properties (<4% in the integral molar values). The numerical differences in the values of the four fitting parameters, A–D, are attributable to the different compositional basis of the activity terms. Regression statistics indicate that the model based on θ provides a slightly better fit to the data. Consequently,

the derived values of x_{max} used in the calculation of θ are approximately correct, and any temperature variation in x_{max} is not resolvable with the existing experimental data. The remaining discussion focuses on the activity model based on θ. Calculated values of the equilibrium constant (using Eq. 12) reproduce the curvature in the experimental values at low temperature and high θ, the relative linearity of the data at high temperature and low θ, the spacing between isotherms (Fig. 6), and the position and curvature of the isotherms (Fig. 7).

DISCUSSION

Thermodynamic quantities

The thermodynamic values (Eq. 12) for hydration of clinoptilolite were estimated from the fit parameters (A, B, C, D) in Eq. 13 using the following relations (where R is the gas constant):

$$\Delta\mu^0_{Hy} = -R(T_0 A + B) \tag{15}$$

$$\Delta\overline{H}^0_{Hy} = -RB \tag{16}$$
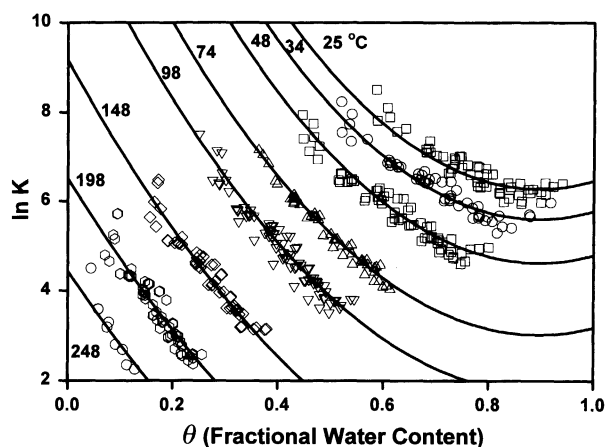
$$\Delta\overline{S}^0_{Hy} = RA \tag{17}$$

FIGURE 6. Comparison of the experimental data for potassium clinoptilolite (symbols) with the calculated fit (solid lines) for water content vs. equilibrium constant at several temperatures. The curves are labeled with the temperatures (in degrees Celsius) of the experiment. The $\ln K$ is defined as $\ln[\theta/(1-\theta)/P]$, and θ is the ratio of the observed water content to the maximum water content at 25 °C.
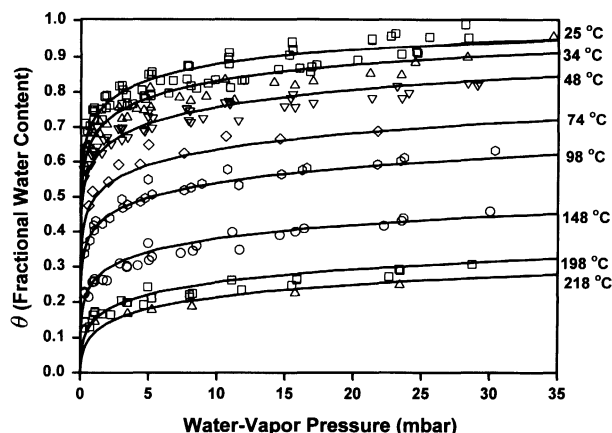
FIGURE 7. Comparison of the experimental data for sodium clinoptilolite (symbols) with the calculated fit (solid lines) for H$_2$O vapor pressure vs. H$_2$O content of clinoptilolite at several temperatures. The curves are labeled with the temperatures of the experiment.

$$W_1 = -RC \tag{18}$$

$$W_2 = -RD. \tag{19}$$

The derived values and their standard errors calculated from the regression (Table 2) are given in Table 3. The partial molar standard states refer to the Henry's law extrapolation to saturation at 25 °C ($\theta = 1$). Additional expressions for the thermodynamics of hydration can be derived from Equation 12 using the relations

$$\overline{H} = \partial\left(\frac{\mu}{T}\right) \bigg/ \partial\left(\frac{1}{T}\right) \tag{20}$$

$$\tilde{H} = \frac{1}{\theta} \int_0^\theta \overline{H}\, d\theta \tag{21}$$

$$\overline{S} = -\left(\frac{\mu}{T} - \frac{\overline{H}}{T}\right) \tag{22}$$

$$\tilde{S} = \frac{1}{\theta} \int_0^\theta \overline{S}\, d\theta. \tag{23}$$

The partial and integral molar enthalpies of hydration as a function of temperature and water content are given by

$$\Delta\overline{H}_{Hy} = \Delta\overline{H}^0_{Hy} + W_1\theta + W_2\theta^2$$
$$+ 3R(T - T_0) \tag{24}$$

$$\Delta\tilde{H}_{Hy} = \Delta\overline{H}^0_{Hy} + \left(\frac{W_1}{2}\right)\theta$$
$$+ \left(\frac{W_2}{3}\right)\theta^2 + 3R(T - T_0). \tag{25}$$

The partial and integral molar entropies of hydration are given by

$$\Delta\overline{S}_{Hy} = \Delta\overline{S}^0_{Hy} + 3R\ln\left(\frac{T}{T_0}\right) - R\ln\left[\frac{\theta}{(1 - \theta)P}\right] \tag{26}$$

$$\Delta\tilde{S}_{Hy} = \Delta\overline{S}^0_{Hy} + 3R\ln\left(\frac{T}{T_0}\right)$$
$$- \frac{R}{\theta}[\theta\ln\theta + (1 - \theta)\ln(1 - \theta) - \theta\ln P]. \tag{27}$$

The integral relations (Eqs. 25 and 27) are written for hydration from an anhydrous state ($\theta = 0$). These equations show that nonideal mixing in the clinoptilolite-H$_2$O system may be modeled solely with excess enthalpy terms while retaining an ideal entropy of mixing. The partial molar Gibbs free energy of hydration is given by Equation 12, and the integral Gibbs free energy of hydration may be obtained from the relation

$$\tilde{G} = \tilde{H} - T\tilde{S}. \tag{28}$$

As observed in other zeolite systems (Barrer and Cram 1971), the highest energy of hydration is associated with calcium clinoptilolite, followed by the Na- and K-bearing varieties, respectively (Table 4). The enthalpy of hydration determined for sodium clinoptilolite is significantly higher, 10–12%, than that found in the calorimetric studies of Barrer and Cram (1971) and Johnson et al. (1991). This difference may reflect greater framework charge in the Fish Creek Mountain clinoptilolite or, more likely, the accuracy of the enthalpy of hydration derived from thermogravimetric data. The enthalpy of hydration for cordierite and that of condensation of water are much lower than that of H$_2$O in clinoptilolite, as expected in systems that do not involve solvation of cations (Carey and Navrotsky 1992). Similarly, the Gibbs free energy and enthalpy of hydration are much greater in analcime (Johnson et al. 1982), as expected from the higher exchangeable-cation to H$_2$O-molecule ratio in analcime. The hydration properties of mordenite determined calorimetrically by Johnson et al. (1992) appear to be very similar to those of clinoptilolite determined in this study.

TABLE 3. Standard-state values for the thermodynamics of hydration in cation-exchanged clinoptilolite

Parameter	Ca-exchanged		Na-exchanged		K-exchanged	
	θ model	std error	θ model	std error	θ model	std error
$\Delta\mu^0_{Hy}$(J/mol)	−79685	2414	−55080	3273	−48949	1171
$\Delta\overline{H}^0_{Hy}$(J/mol)	−120477	2232	−99593	2910	−91183	1031
$\Delta\overline{S}^0_{Hy}$[J/(mol·K)]	−136.82	3.08	−149.30	5.03	−141.65	1.86
W_1(J/mol)	137070	3332	72214	34123	74649	1277
W_2(J/mol)	−74935	2129	−32111	2248	−41726	920

Note: Errors derived from regression analysis. The values (except entropy) are used in Equation 12. Excess significant figures are retained for calculations.

TABLE 4. Molar values of the thermodynamics of hydration for cation-exchanged clinoptilolite determined in this study compared with values measured in clinoptilolite, other zeolites, and H_2O

| Material	$\Delta \bar{G}_{Hy}$ (kJ/mol H_2O)	$\Delta \bar{H}_{Hy}$ (kJ/mol H_2O)	$\Delta \bar{S}_{Hy}$ (J/mol H_2O/K)
Ca-Cpt (1)	-36.13 ± 3.02	-76.92 ± 2.88	-136.8 ± 3.1
Na-Cpt (1)	-29.68 ± 3.77	-74.19 ± 3.46	-149.3 ± 5.0
K-Cpt (1)	-25.53 ± 1.37	-67.78 ± 1.25	-141.7 ± 1.9
Sodic-Cpt (2)	n.d.	-65.5	n.d.
Na-Cpt (3)	n.d.	-66.1	n.d.
H_2O (4)	-8.57	-44.02	-118.9
Cordierite (5)	-9.5	-41.8	-108.2
Analcime (6)	-44.9	-84.9	-133.8
Mordenite (7)	-33.5	-73.8	-134.8

Note: The values were obtained using Equations 25, 27, and 28 with θ = 1. References given in parentheses: 1 = this study, 2 = Johnson et al. (1991) adiabatic and solution calorimetry, 3 = Barrer and Cram (1971) immersion calorimetry, 4 = Robie et al. (1979), 5 = Carey (1995) phase equilibria, 6 = Johnson et al. (1982) adiabatic and solution calorimetry, and 7 = Johnson et al. (1992) adiabatic and solution calorimetry. Uncertainties were derived from the standard errors of the regression coefficients; n.d. = not determined.

H_2O content and enthalpy of hydration

Equilibrium H_2O contents of clinoptilolite as a function of temperature and pressure may be calculated using Equation 12 and the values in Table 3. This calculation requires an iterative approach to find the value of θ consistent with a given pressure and temperature. The partial molar enthalpy of hydration may be calculated using Equation 24. The partial molar enthalpies increase with decreasing H_2O content for each cation-exchanged clinoptilolite, as observed in other zeolites (Fig. 8; Barrer and Cram 1971). As discussed by Carey and Navrotsky (1992), the partial molar enthalpies of zeolites are expected to converge to similar values as saturation is approached because the exchangeable cations are effectively screened by previously sorbed H_2O molecules. Consistent with this prediction, all three cation types have the same partial molar enthalpy at $\theta = 1$ within the uncertainty of the determination (Fig. 8). Similarly, the increase in the partial molar enthalpies with decreasing θ is expected from increasing interaction with exchangeable cations. The relative sequence of enthalpies at low θ, with Ca > Na > K, is consistent with the work of Barrer and Cram (1971) and may be expected from the energetics of solvation of the exchangeable cations.

PHASE EQUILIBRIA INVOLVING CLINOPTILOLITE

To evaluate equilibria involving clinoptilolite, an expression for the activity of clinoptilolite as a function of H_2O content must be developed. Rewriting Equation 1 as

$$H_2O + \text{anhydrous clinoptilolite} = \text{clinoptilolite} \cdot H_2O \tag{29}$$
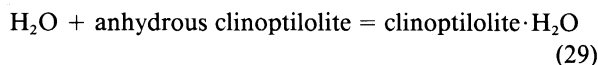
makes it apparent that the activity of H_2O in clinoptilolite (Eq. 10) is equivalent to the ratio of the activities of hydrous and anhydrous clinoptilolite (HyCpt and AnhyCpt):
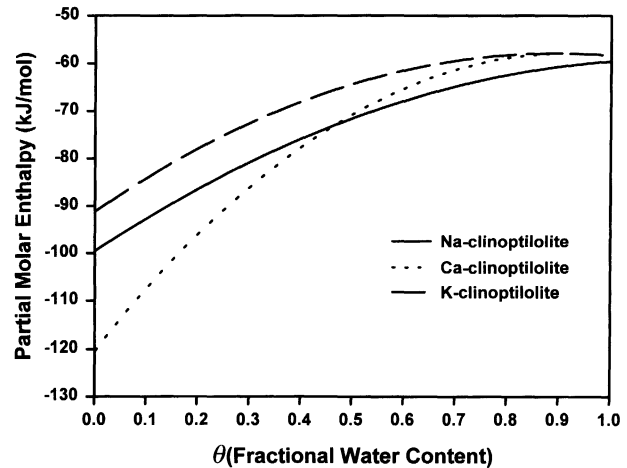

FIGURE 8. Calculated curves of the partial molar enthalpies of hydration of sodium, calcium, and potassium clinoptilolite at 25 °C.

$$a_{H_2O}^{Cpt} = \frac{a_{HyCpt}^{Cpt}}{a_{AnhyCpt}^{Cpt}} = \frac{\gamma_{HyCpt}^{Cpt}\theta}{\gamma_{AnhyCpt}^{Cpt}(1 - \theta)}. \tag{30}$$

The ideal activities of hydrous and anhydrous clinoptilolite are θ and $(1 - \theta)$, respectively.

A formulation of the nonideality in hydrous and anhydrous clinoptilolite that is consistent with the nonideality of H_2O in clinoptilolite (Eq. 10) can be obtained using an asymmetric Margules formulation. The Gibbs free energy of the asymmetric solution is given by

$$G^{Cpt} = \theta\mu_{HyCpt}^{0,Cpt} + (1 - \theta)\mu_{AnhyCpt}^{0,Cpt}$$
$$+ RT[\theta \ln\theta + (1 - \theta)\ln(1 - \theta)]$$
$$+ [\alpha(1 - \theta) + \beta\theta]\theta(1 - \theta) \tag{31}$$

(cf. Thompson 1967), where α and β are the mixing parameters. Chemical potentials of hydrous and anhydrous clinoptilolite derived from Equation 31 are

$$\mu_{HyCpt}^{Cpt} = \mu_{HyCpt}^{0,Cpt} + RT \ln \theta + (1 - \theta)^2(2\beta - \alpha)$$
$$+ (1 - \theta)^3(2\alpha - 2\beta) \tag{32}$$

$$\mu_{AnhyCpt}^{Cpt} = \mu_{AnhyCpt}^{0,Cpt} + RT \ln(1 - \theta) + \theta^2(2\alpha - \beta)$$
$$+ \theta^3(2\beta - 2\alpha). \tag{33}$$

Consistency of the activity expression for H_2O (Eq. 10) with Equations 32 and 33 requires the following relationships between the two sets of mixing parameters:

$$\alpha = -\tfrac{1}{2}W_1 - \tfrac{1}{3}W_2 \tag{34}$$

$$\beta = -\tfrac{1}{2}W_1 - \tfrac{2}{3}W_2. \tag{35}$$

Equations 33–35 provide the basis for the evaluation of reactions involving clinoptilolite, assuming that an expression for $\mu_{AnhyCpt}^{0,Cpt}$ exists.

As an example, the following equilibrium is considered:

$$8 SiO_2 \text{ (quartz)} + 7 NaAlSi_3O_8 \text{ (albite)}$$
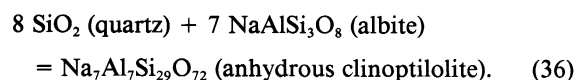$$= Na_7Al_7Si_{29}O_{72} \text{ (anhydrous clinoptilolite)}. \tag{36}$$

TABLE 5. Thermodynamic properties of sodic clinoptilolite based on the measurements of Johnson et al. (1991)

Property*	$\theta = 0.905$**	$\theta = 1$†	$\theta = 0$†	$\theta = 0$‡
ΔG_f^0(kJ/mol)	−38156.8	−38698.3	−32464.2	−32569.0
ΔH_f^0(kJ/mol)	−41290.0	−41982.9	−34354.6	−34534.8
S^0[J/(mol·K)]	2966.1	2993.8	2039.5	1789.6

* Gibbs free energy and enthalpy of formation from the elements and the third-law entropy.
** Calorimetric measurements of Johnson et al. (1991) on hydrous sodic clinoptilolite.
† Calculated thermodynamic properties of fully hydrous and anhydrous clinoptilolite based on Johnson et al. (1991) data for $\theta = 0.905$, Equations 25 and 27, and thermodynamic data for water vapor (Robie et al. 1979).
‡ Calorimetric values reported by Johnson et al. (1991) for anhydrous sodic clinoptilolite. Note that Johnson et al. determined ΔH_f^0 directly and assumed that the entropy of H₂O in clinoptilolite was the same as that measured for mordenite in the calculation of S^0 and ΔG_f^0.

The thermodynamic properties of anhydrous clinoptilolite may be derived from calorimetric data for hydrous clinoptilolite (Johnson et al. 1991). Johnson et al. (1991) measured the Gibbs free energy of formation of a sodic clinoptilolite equilibrated with a 50% relative humidity atmosphere at 20 °C. The sodic clinoptilolite had 21.84 H₂O per formula unit (72 framework O atoms pfu). In the analysis that follows, it is assumed that the thermodynamics of hydration measured for the Na-exchanged clinoptilolite apply to the sodic clinoptilolite of Johnson et al. (1991). The H₂O content of the sodic clinoptilolite, predicted by Equation 12 using the values in Table 3, is 22.04 H₂O; this compares well with that given by Johnson et al. (1991). With $\theta = 0.905$, the thermodynamic properties of anhydrous and fully hydrous sodic clinoptilolite can be calculated by application of the integral relations in Equations 25 and 27 and correcting for the thermodynamic properties of water vapor (Table 5). The enthalpy of formation of anhydrous clinoptilolite measured by Johnson et al. (1991) may be compared directly with that calculated from the hydration data (Table 5). The difference, 8.3 kJ/mol H₂O, reflects the higher energetics of hydration determined in this study. The data in Table 5 in combination with the formulation in Equation 33 and the relationships in Equations 34 and 35 provide the thermodynamic properties of anhydrous clinoptilolite.

Equilibrium for the reaction in Equation 36 was calculated using the heat capacity of anhydrous clinoptilolite (Johnson et al. 1991), molar volume of clinoptilolite (126.26 J/bar; Armbruster and Gunter 1991), thermodynamic data for quartz and low albite (Robie et al. 1979), thermodynamic data for H₂O (Haar et al. 1984), and the data in Table 5. (This calculation is intended to illustrate the application of the hydration results and is inaccurate to the extent that calorimetric data of Johnson et al. (1991) apply to a natural, sodic clinoptilolite with a composition different from that in Eq. 36.) These data result in a reaction for the breakdown of sodium clinoptilolite to albite that lies well within the steam field (curve labeled "Na-H₂O" in Fig. 9).
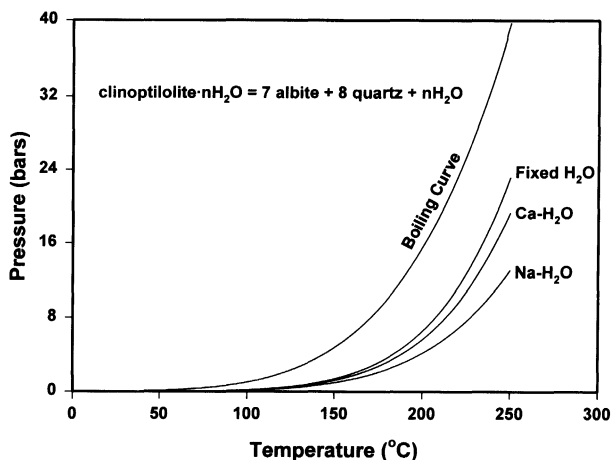

FIGURE 9. Calculation of the breakdown of hydrous clinoptilolite to an assemblage of low albite, quartz, and H₂O. The curves labeled "Na-H₂O" and "Ca-H₂O" were obtained using the hydration energetics measured for the Na- and Ca-exchanged clinoptilolite, respectively. The curve labeled "Fixed H₂O" assumed a constant H₂O content. Also given is the boiling curve for water.

Two additional calculations were made: The first used the thermodynamic properties of hydrous clinoptilolite as measured by Johnson et al. (1991) but kept the water content fixed at 21.84 H₂O pfu (curve labeled "Fixed H₂O"); and the second used the hydration energetics of Ca-exchanged clinoptilolite (curve labeled "Ca-H₂O"). These calculations illustrate how partial dehydration stabilizes clinoptilolite relative to the assumption of a fixed H₂O content. For example, the amount of H₂O in clinoptilolite along the Na-H₂O breakdown curve decreases from $\theta = 0.77$ to 0.61 (i.e., from 18.6 to 14.7 H₂O pfu). The assumption of a fixed H₂O content results in a reasonable approximation at temperatures below 150 °C but differs from the Na-H₂O curve by 10 bars at 250 °C. Similarly, the hydration energetics appropriate for calcium clinoptilolite destabilize clinoptilolite because of the greater amount of H₂O in the structure. Generalization of these observations to other zeolites requires caution because the magnitude of the difference in the stability curves of Figure 9 is a function of the H₂O content of the zeolite and the thermodynamics of hydration.

APPLICATION TO YUCCA MOUNTAIN

A thermohydrologic model of the evolution of Yucca Mountain following the emplacement of nuclear waste is being developed as part of site characterization. The effect of clinoptilolite on the thermal and hydrologic evolution may be significant because of the dehydration-hydration reactions that occur as temperature and H₂O vapor pressure change. Dehydration absorbs thermal energy and tends to depress temperatures in areas with significant concentrations of clinoptilolite or other hydrous minerals. It also releases an amount of water in the unsaturated zone that is significant relative to the total amount of water contained in the rocks.
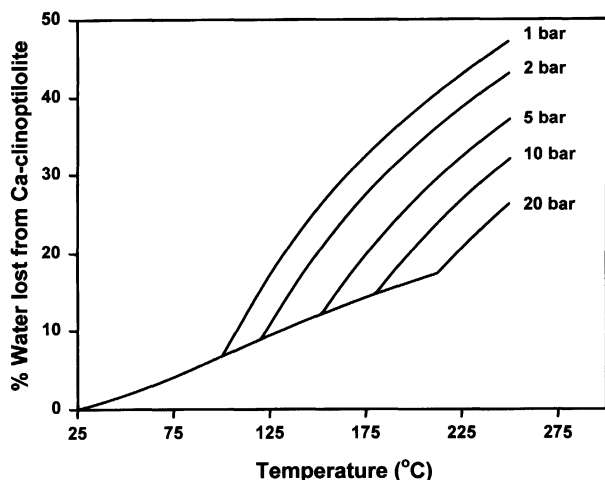
FIGURE 10. Calculated dehydration evolution of calcium clinoptilolite under conditions of rising temperature and differing maximum pressures. Dehydration occurs along the boiling curve until the maximum pressure is reached.

FIGURE 11. Calculated thermal and hydrologic evolution of a 1 m³ block of potassium clinoptilolite with 10% porosity, insulated boundaries, maximum H₂O vapor pressure of 1 bar, and 14 W of thermal energy. The two solid lines show the temperature of a block of potassium clinoptilolite that dehydrates and one that does not dehydrate. The dotted line shows the water content of the clinoptilolite in the dehydrating block.

This experimental work provides the means of assessing these effects. The first example explores the effect of total pore pressure on the degree of dehydration as temperature rises in clinoptilolite-bearing rocks. H_2O vapor pressure increases along the boiling curve until the maximum sustainable pressure is achieved in the pore system. The maximum pressure depends on factors such as the permeability of the rocks and the heating rate. To illustrate the effect, the relative water content of calcium clinoptilolite was calculated as a function of maximum pore pressures of 1, 5, 10, and 20 bars and from 25 to 250 °C (Fig. 10). Dehydration occurs even while the temperature rises along the boiling curve, but the amount of dehydration increases significantly after the maximum pore pressure is achieved. The degree of dehydration at 200 °C depends on the maximum pore pressure and differs by 26% between 1 and 20 bar. The sodium and potassium clinoptilolite results are similar, except that slightly more water is lost than for calcium clinoptilolite.

The second example illustrates the effect of dehydration on temperature and pore saturation. This simplified model considers the thermal and hydrologic evolution of a thermally insulated block of pure clinoptilolite that receives a constant source of thermal energy. Although this is not a good model for the thermal evolution of zeolitic rocks at Yucca Mountain (because these are not thermally insulated), it illustrates the effect of dehydration processes. In the model, a 1 m³ box has 10% porosity, is initially at 25° C, 100% relative humidity, and receives a thermal flux of 14 W while maintaining a uniform temperature (the value of the thermal flux is representative of those considered for Yucca Mountain). The thermal flux is consumed by the heat capacity of clinoptilolite and by the dehydration processes. It is assumed that the box is porous to water vapor and a maximum pressure of 1 bar is attained. The heat capacity used for anhydrous clinoptilolite is that of Johnson et al. (1991). The heat
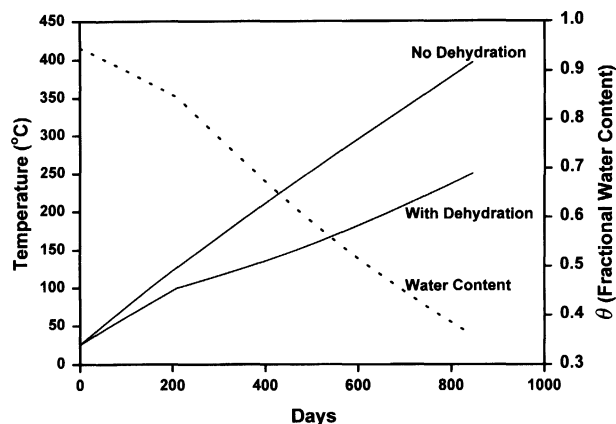
capacity of hydrous clinoptilolite is taken as the sum of the heat capacities of anhydrous clinoptilolite, H_2O vapor (Robie et al. 1979), and 3R (cf. the discussion in Data Analysis; Carey 1993).

There is a dramatic difference in temperature evolution between a box of potassium clinoptilolite that does not dehydrate and one that does (Fig. 11). Dehydration suppressed temperature evolution markedly. The model without dehydration reached 395 °C after 844 d, whereas that with dehydration reached only 250 °C over the same period. The kink in the temperature evolution at 100 °C is the point at which the pores attained the maximum H_2O vapor pressure of 1 bar. During the dehydration process, the potassium clinoptilolite released 1.63 pore volumes of water (assuming 10% porosity and 1 g/cm³ density). In other words, the model constraints require that an amount of water equal to 16% of the rock volume must drain away. The Ca- and Na-exchanged clinoptilolite behaved similarly, requiring, respectively, 877 and 935 d to reach 250 °C in the model with dehydration in comparison with 410 and 433 °C for the nondehydrating case.

ACKNOWLEDGMENTS

REFERENCES CITED

Alberti, A. (1975) The crystal structure of two clinoptilolites. Tschermaks Mineralogische und Petrographische Mitteilungen, 22, 25–37.
Armbruster, T., and Gunter, M.E. (1991) Stepwise dehydration of heu-

landite-clinoptilolite from Succor Creek, Oregon, U.S.A.: A single-crystal X-ray study at 100 K. American Mineralogist, 76, 1872–1883.

Barrer, R.M. (1978) Zeolites and clay minerals as sorbents and molecular sieves, 497 p. Academic, London, U.K.

Barrer, R.M., and Fender, B.E.F. (1961) The diffusion and sorption of water in zeolites: II. Sorption. Journal of the Physics and Chemistry of Solids, 21, 1–11.

Barrer, R.M., and Davies, J.A. (1970) Sorption in decationated zeolites: I. Gases in hydrogen chabazite. Proceedings of the Royal Society of London, A320, 289–308.

Barrer, R.M., and Cram, P.J. (1971) Heats of immersion of outgassed and ion-exchanged zeolites. In E.M. Flanigen and L.B. Sand, Eds., Molecular sieve zeolites (vol. II), p. 105–131. American Chemical Society, Washington, DC.

Bish, D.L. (1984) Effects of exchangeable cation composition on the thermal expansion/contraction of clinoptilolite. Clays and Clay Minerals, 32, 444–452.

——— (1990) Long-term thermal stability of clinoptilolite: The development of a "B" phase. European Journal of Mineralogy, 2, 771–777.

Carey, J.W. (1993) The heat capacity of hydrous cordierite above 295 K. Physics and Chemistry of Minerals, 19, 578–583.

——— (1995) A thermodynamic formulation of hydrous cordierite. Contributions to Mineralogy and Petrology, 119, 155–165.

Carey, J.W., and Navrotsky, A. (1992) The molar enthalpy of dehydration of cordierite. American Mineralogist, 77, 930–936.

Chipera, S.J., Guthrie, G.D., Jr., and Bish, D.L. (1993) Preparation and purification of mineral dusts. In G.D. Guthrie, Jr. and B.T. Mossman, Eds., Health effects of mineral dusts, p. 235–249. Mineralogical Society of America, Washington, DC.

Gottardi, G., and Galli, E. (1985) Natural zeolites, 409 p. Springer-Verlag, Berlin.

Haar, L., Gallagher, J.S., and Kell, G.S. (1984) NBS/NRC steam tables: Thermodynamic and transport properties and computer programs for vapor and liquid states of water in SI units, 320 p. Hemisphere Publishing, Washington, DC.

Johnson, G.K., Flotow, H.E., O'Hare, P.A.G., and Wise, W.S. (1982) Thermodynamic studies of zeolites: Analcime and dehydrated analcime. American Mineralogist, 67, 736–748.

Johnson, G.K., Tasker, I.R., Jurgens, R., and O'Hare, P.A.G. (1991) Thermodynamic studies of zeolites: Clinoptilolite. Journal of Chemical Thermodynamics, 23, 475–484.

Johnson, G.K., Tasker, I.R., Flotow, H.E., O'Hare, P.A.G., and Wise, W.S. (1992) Thermodynamic studies of mordenite, dehydrated mordenite, and gibbsite. American Mineralogist, 77, 85–93.

Robie, R.A., Hemingway, B.S., and Fisher, J.R. (1979) Thermodynamic properties of minerals and related substances at 298.15 K and 1 bar (10⁵ Pascals) pressure and at higher temperature, 456 p. U.S. Geological Survey Bulletin, 1452.

Simonot-Grange, M.H. (1979) Thermodynamic and structural features of water sorption in zeolites. Clays and Clay Minerals, 27, 423–428.

Thompson, J.B., Jr. (1967) Thermodynamic properties of simple solutions. In P.H. Abelson, Ed., Researches in geochemistry (vol. II), p. 340–361. Wiley, New York.

Yamanaka, S., Malla, P.B., and Komarneni, S. (1989) Water sorption and desorption isotherms of some naturally occurring zeolites. Zeolites, 9, 18–22.